BMC Biology

RESEARCH ARTICLE

Open Access

The roles of cell wall polysaccharides in response to waterlogging stress in *Brassica napus* L. root

Jijun Li[1,2†], Yuting Zhang[1†], Yahui Chen[1,3], Yijing Wang[1], Zhihua Zhou[1], Jinxing Tu[1], Liang Guo[1,4,5] and Xuan Yao[1,5*]

Abstract

Background *Brassica napus* L. (*B. napus*) is susceptible to waterlogging stress during different cultivation periods. Therefore, it is crucial to enhance the resistance to waterlogging stress to achieve a high and stable yield of *B. napus*.

Results Here we observed significant differences in the responses of two *B. napus* varieties in root under waterlogging stress. The sensitive variety (23651) exhibited a more pronounced and rapid reduction in cell wall thickness and root integrity compared with the tolerant variety (Santana) under waterlogging stress. By module clustering analysis based on transcriptome data, we identified that cell wall polysaccharide metabolism responded to waterlogging stress in root. It was found that pectin content was significantly reduced in the sensitive variety compared with the tolerant variety. Furthermore, transcriptome analysis revealed that the expression of two homologous genes encoding polygalacturonase-inhibiting protein 2 (PGIP2), involved in polysaccharide metabolic pathways, was highly upregulated in root of the tolerant variety under waterlogging stress. *BnaPGIP2s* probably confer waterlogging resistance by inhibiting the activity of polygalacturonases (PGs), which in turn reduces the degradation of the pectin backbone polygalacturonic acid.

Conclusions Our findings demonstrate that cell wall polysaccharides in root plays a vital role in response to the waterlogging stress and provide a theoretical foundation for breeding waterlogging resistance in *B. napus* varieties.

Keywords *Brassica napus*, Waterlogging stress, Root, Cell wall polysaccharides, *BnaPGIP2*

Background

Waterlogging is one of the major abiotic stresses in crops, as it can cause damage or even be fatal for plant growth and development due to poor soil water permeability and surface drainage. The occurrence of waterlogging is often caused by extreme rainfall, soil hardening, and poor field drainage [1]. Approximately 10% of the world's arable land is affected by varying degrees of waterlogging, resulting in yield loss ranging from 15% to 80% [2].

When the soil is waterlogged, O_2 in the pore space is replaced by water [3–5]. The living activities of microorganism and plant root further consume the residual O_2, leading to a rapid decline in soil O_2 content. This forces

†Jijun Li and Yuting Zhang contributed equally to this work.

*Correspondence:
Xuan Yao
xuanyao@mail.hzau.edu.cn
[1] National Key Laboratory of Crop Genetic Improvement, Huazhong Agricultural University, Wuhan 430070, China
[2] Guizhou Institute of Oil Crops, Guizhou Academy of Agricultural Sciences, Guiyang 550006, China
[3] Chengde Academy of Agricultural and Forestry Sciences, Chengde 067000, China
[4] Hubei Hongshan Laboratory, Wuhan 430070, China
[5] Yazhouwan National Laboratory, Sanya 572025, China

the plants to rapidly enter a hypoxic state. The plant root is most directly exposed to soil water, and the cell wall serves as the first barrier against biotic and abiotic stresses. The cell wall plays a crucial role in maintaining cell expansion, integrity, and intercellular signal communication [6, 7]. Alterations in root cell wall ultrastructure can occur due to waterlogging, and stable intercellular and intracellular structures in root help maintain tolerance to waterlogging stress [8, 9]. Under waterlogging conditions, the sub-environmental hypoxia could promote the synthesis of ethylene, and the ethylene accumulation in the roots surrounded by water would induce programmed cell death (PCD) in the cortical tissues [10–12]. Therefore, it is particularly worth to investigate the mechanisms of stress changes in plant root cell wall.

Structural polysaccharides, cellulose, hemicellulose and pectin, are main components of cell wall [13, 14]. Previous studies have also shown that during cell wall degradation under biotic stress, changes in the cell wall are caused by the polysaccharide fractions and are accomplished by regulating the cross-linking between cellulose, lignin, and pectin polymers [15]. Many enzymes related to modification of cell wall polysaccharides are also involved in alteration of cell-wall structure, including xyloglucan endotransglycosylase (XET), expansin, cellulase, and pectinase [16–19]. Polygalacturonases (PGs), a type of pectinases, catalyze the cleavage of the pectin backbone polygalacturonic acid, leading to the degradation of pectin. Previous studies have shown that polygalacturonase-inhibiting proteins (PGIPs) inhibit the activity of PGs by specifically binding to PGs secreted by pathogens, thereby reducing pectin degradation in the cell wall [20, 21]. Cell wall-related genes also have been identified to respond to waterlogging stress in different species by comparative transcriptome analysis, including *copper amine oxidase* (*CuAO*), *pectin methylesterase* (*PME*) [22, 23]. However, how cell wall polysaccharide biosynthesis in root participates in the response to waterlogging stress remains unclear.

Brassica napus L. (*B. napus*) is an important oil crop in the world. Waterlogging will lead to impaired root development, thus affecting the normal growth of the above-ground part following with weakened plant photosynthesis and leaf senescence, which even leads to the plant death and significant yield reduction at maturity [24–27]. *B. napus* plants at vegetative developmental stages, such as radical elongation and seedling stages, are more sensitive to waterlogging stress than generative stages [25]. More than 3-day waterlogging stress at seedling stage will significantly affect seed yield at maturity in *B. napus* [28]. Two-weeks waterlogging stress at seedling stage can result in a 20% to 50% loss in seed yield of *B. napus* [24, 28, 29]. Therefore, analyzing the dynamic changes and gene expression regulation of *B. napus* in response to waterlogging at seedling stage will help to deepen understanding the response mechanism of waterlogging and lay a foundation for genetic improvement for cultivating waterlogging-resistant *B. napus* varieties.

In this study, waterlogging treatments were performed on *B. napus* tolerant (Santana) and sensitive (23,651) varieties, which exhibited significantly different changes in root growth, physiological response and gene regulation under waterlogging stress. Transcriptome analysis were used to identify waterlogging-related metabolic pathways. Function analysis of key genes validated that the pectin metabolism was involved in responses to waterlogging stress in *B. napus*. We thus aimed to investigate the response of the *B. napus* root under waterlogging stress, and to explore possible strategies to cope with waterlogging stress.

Results

The different responses of tolerant and sensitive *B. napus* varieties to waterlogging stress

In our previous studies, it was discovered that 'Santana' is tolerant to flooding, while '23,651' is sensitive to flooding during the germination stage [30]. To examine the response of *B. napus* to waterlogging stress at the seedling stage, we selected 'Santana' as an extreme waterlogging-tolerant variety and '23,651' as an extreme waterlogging-sensitive variety for further study. Under normal conditions (CK), both varieties had similar root growth. However, after 7 days of waterlogging (WL), the growth inhibition in the sensitive variety was significantly more severe (Fig. 1a). Furthermore, the shoot fresh weight and root fresh weight of the sensitive variety were significantly reduced compared to the tolerant variety after the waterlogging treatment (Fig. 1b).

The root of *B. napus* is the most susceptible organ to waterlogging stress and responds directly to the stress. Therefore, we focused on the changes in the root under waterlogging stress in *B. napus*. We investigated the degree of damage to the *B. napus* root tip caused by prolonged waterlogging stress. Evens Blue staining was then used to assess cell membrane integrity and the degree of damage in root tip cells. In the absence of waterlogging stress, the cell membrane was intact and staining was not prominent. However, after 10 to 12 h of waterlogging, the root tip of the sensitive variety showed obvious damage, and after 3 days of waterlogging, the cells began to collapse and dissociate. In contrast, the root of the tolerant variety showed damage after 1 day of waterlogging, and the cell membrane remained relatively intact even after 3 days of waterlogging (Fig. 1c). Additionally, Nitro Blue Tetrazolium (NBT) staining was performed on the root tip of both varieties. It was observed that under normal

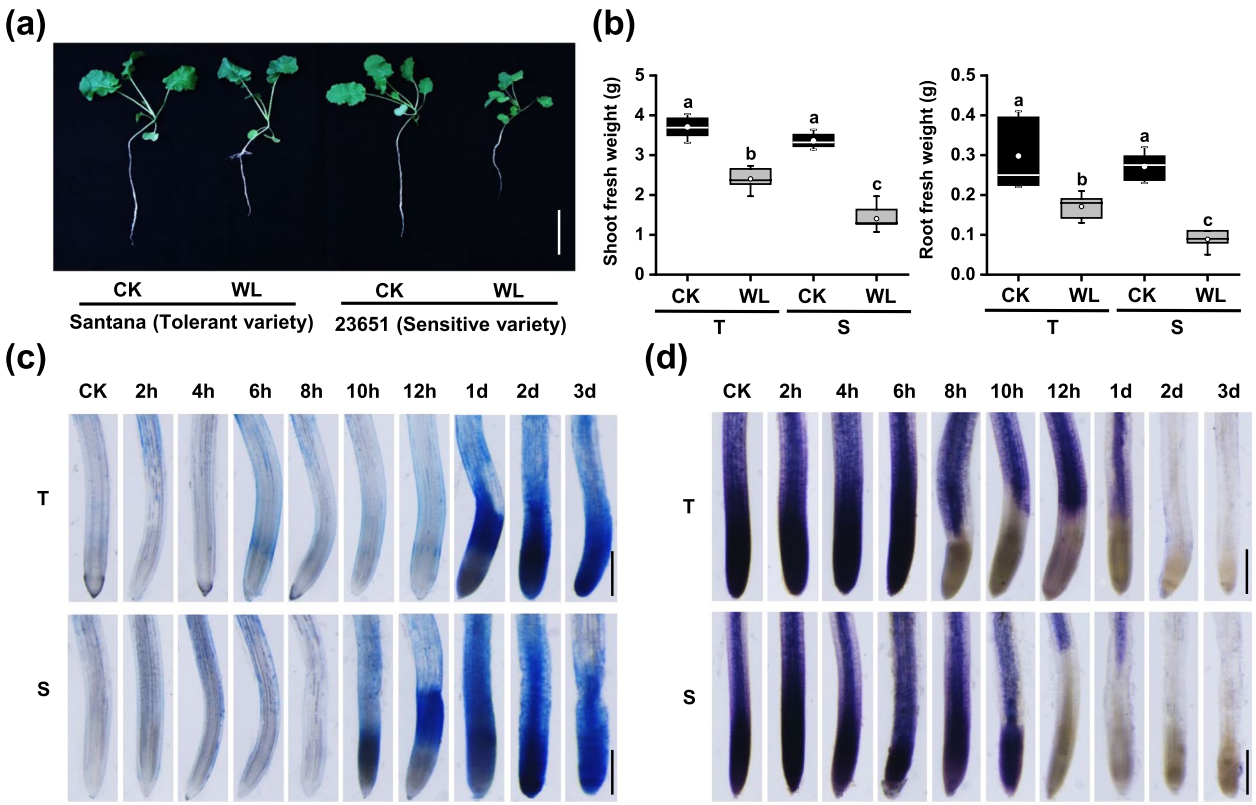

Fig. 1 The phenotypes of waterlogging tolerance and waterlogging sensitivity in *B. napus* varieties under waterlogging stress. **a** Growth of waterlogging tolerant (T) and sensitive (S) *B. napus* varieties under normal conditions (CK) and waterlogging (WL) for 7 days at 2-leaf stage. Bar = 5 cm. **b** Changes in shoot fresh weight and root fresh weight of waterlogged tolerant and sensitive *B. napus* varieties under CK and waterlogging conditions. Different letters indicate significant differences, while the same letters indicate no significant difference (n = 10, one-way ANOVA for multiple comparisons, $P < 0.05$). **c** Detection of cell membrane integrity by Evans Blue staining in root tips of waterlogging tolerant and sensitive *B. napus* varieties under CK and WL. Bars = 1 mm. **d** Measurement of $O_2^{\cdot-}$ content in root tips of waterlogging tolerant and sensitive *B. napus* varieties by Nitro Blue Tetrazolium (NBT) staining under CK and WL. Bars = 1 mm

conditions, the root tips of both varieties were metabolically active and produced a certain level of $O_2^{\cdot-}$ (Fig. 1d). However, as the duration of waterlogging increased, the root cells gradually died and the level of $O_2^{\cdot-}$ decreased. After 12 h of waterlogging, the metabolic activity of root cells in the tolerant variety was normal and the level of $O_2^{\cdot-}$ remained relatively stable. In contrast, the sensitive variety exhibited impaired metabolic activity, resulting in a significant decrease in staining signals (Fig. 1d). Therefore, the results indicate that differential waterlogging tolerance between these two varieties may be attributed to the integrity and function of the root system.

Transcriptome analysis identified waterlogging-related metabolic pathways

To investigate the underlying genetic basis contributing to the contrasting root responses of the two materials under waterlogging conditions, transcriptome analysis was conducted to discern genetic differences between them. A total of three biological repetitions were performed at two treatment time points (12 h and 72 h) at the 2-leaf stage, corresponding to the roots of two *B. napus* lines (S, T), resulting in a total of 18 samples. Approximately ~ 60 Gb raw data were obtained. After quality control and filtering low-quality reads, high-quality reads were obtained, with an average of 95.57% of the reads being successfully mapped to the *B. napus* reference genome. Approximately 4.43% of the total reads were not matched due to stringent screening parameter settings, sequencing assembly errors, or an incomplete reference genome. Furthermore, both the heat map and PCA plot revealed that the gene expression correlations between biological repetitions of samples were above 90%, indicating a high level of reproducibility and confidence in the data (Additional file 1: Figure S1). For the transcriptome data, the differentially expressed genes (DEGs) in roots were identified based on the criteria of a P-value < 0.05 and |log2foldchange| > 1 (Additional file 2: Table S1, 2).

The results of transcriptome analysis revealed a significant increase in the number of DEGs in response to waterlogging stress, which was correlated with the duration of the waterlogging treatment (Fig. 2a; Additional file 2: Table S1-2). This could be attributed to the fact that the root is the most direct and sensitive organ to waterlogging damage in *B. napus*. In order to obtain a comprehensive expression profile of DEGs in *B. napus* roots under waterlogging stress, we conducted mclust analysis on 19,587 DEGs and divided them into 20

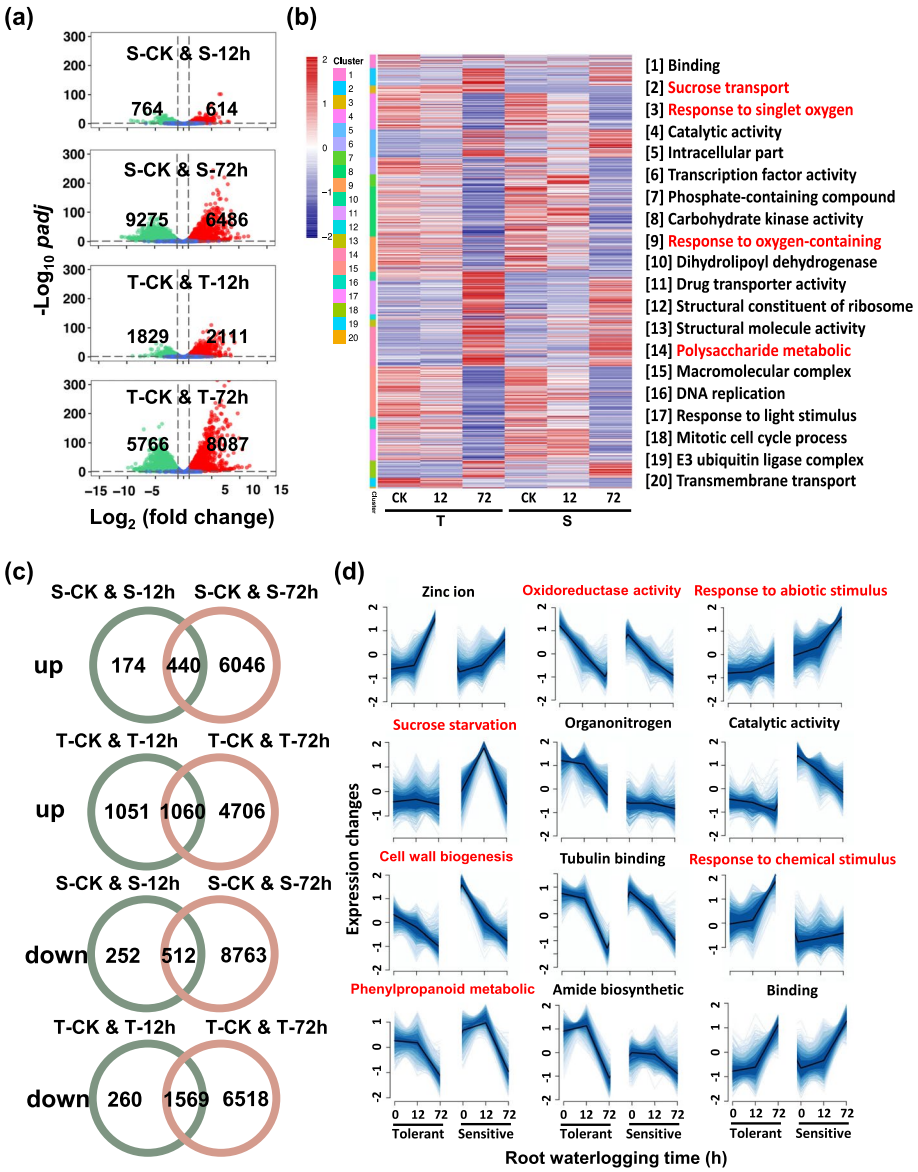

Fig. 2 Identification of differentially expressed genes (DEGs) and module division by transcriptome analysis. **a** Volcano map of DEGs compared with normal conditions (CK) and under waterlogging (WL) of *B. napus* roots. Red dots represent up-regulated genes, green dots represent down-regulated genes, and blue dots represent non-differentially expressed genes. The X-axis represents the fold change of difference after conversion to log2, and the Y-axis represents the significance value after conversion to -log10. **b** Mclust clustering heatmap of DEGs in the root. Heat map of DEGs clustered under different time points (12 h, 72 h) of waterlogged root, and the pathways with FDR < 0.05 and associated with waterlogged metabolism or the most significantly enriched pathway in each cluster are indicated. **c** Venn diagram of up-regulated and down-regulated DEGs in the roots of sensitive (S) and tolerant (T) *B. napus* varieties under WL at different time points. Each circle represents a set of gene sets. The overlapping areas of different circles represent DEGs common to the gene sets. Non-overlapping parts represent uniquely DEGs. The numbers in the figure represent the number of DEGs in the corresponding regions. **d** Mfuzz time clusters of DEGs in the root. Time clusters of DEGs in *B. napus* root at different time points (12 h, 72 h) under WL. The pathways with FDR < 0.05 and associated with waterlogged metabolism or the most significantly enriched pathway for each cluster gene in GO enrichment analysis are indicated

clusters. Additionally, we performed GO enrichment analysis on the biological processes of gene expression in each cluster. The pathways (FDR < 0.05) that were related to waterlogging stress or deemed significant in the GO enrichment analysis were marked for each cluster (Fig. 2b). Notably, clusters 2, 3, 9, and 14 exhibited biological processes that correspond to waterlogging stress in *B. napus* roots (Fig. 2b). For instance, clusters 2 and 14 were enriched in polysaccharide metabolic processes, disaccharide transport, and sucrose synthesis pathways (Additional file 1: Figure S2a-b; Additional file 2: Table S3, 4), while clusters 3 and 9 were enriched in singlet oxygen, oxygen-containing compounds, carbohydrate metabolism, and multiple pathways responsive to waterlogging injury (Additional file 1: Figure S2c-d; Additional file 2: Table S5, 6).

Furthermore, in both the tolerant and sensitive varieties, more genes were specifically down-regulated in the root. However, when compared to the control (CK), there were more genes regulated after 72 h of waterlogging in the tolerant variety, with the number of down-regulated genes being lower than that of up-regulated genes in the root (Fig. 2c). To obtain transcriptome time series characteristic expression profiles, we clustered genes with similar expression patterns through mfuzz clustering analysis to understand the biological dynamic patterns and functions of these genes. The gene expression matrices of the root were divided into 12 clusters, each representing a different gene expression pattern (Fig. 2d). All clusters in the root exhibited similar change trends in expression patterns between the tolerant and sensitive varieties under the same treatment, although the expression of genes in some modules differed slightly between the two varieties (Fig. 2d). Moreover, GO enrichment analysis was conducted on the biological processes of gene expression in each cluster. Under waterlogging conditions, many physiological and metabolic activities tend to be slowed down, such as oxidoreductase activity, organo nitrogen, catalytic activity, cell wall biogenesis, tubulin binding, phenylpropanoid metabolic, and amide biosynthetic processes (Fig. 2d). Conversely, metabolic processes associated with abiotic stress resistance were up-regulated, including zinc ion, response to abiotic stimulus, sucrose starvation, response to chemical stimulus, and binding (Fig. 2d). Cluster 2 and cluster 4 were primarily enriched in metabolic processes such as oxidoreductase activity, ATPase activator activity, and sugar starvation, which could be attributed to the anaerobic or anoxic condition induced by waterlogging stress, forcing the plants to limit aerobic respiration and energy production to sustain vital activity (Additional file 1: Figure S3a, b; Additional file 2: Table S7, 8). Genes in cluster 3 and cluster 9 predominantly responded to abiotic stimuli, and the expression patterns of genes in cluster 9 showed significant differences between the sensitive and tolerant varieties (Fig. 2d). Specifically, the sensitive variety exhibited consistent and smooth growth trends after 12 and 72 h of treatment, whereas no sudden increase in gene expression was observed in the tolerant variety after 72 h (Additional file 1: Figure S3c, d; Additional file 2: Table S9, 10). Furthermore, it was observed that genes in cluster 7 and cluster 10 were mainly enriched in cell wall synthesis, hemicellulose metabolic processes, secondary metabolic genes and phenylpropanoid metabolic processes (Fig. 2d; Additional file 1: Figure S3e, f). Additionally, the activity of cellulases, pectinases, and xylanases, may be involved in root cell wall biosynthesis under waterlogging stress (Additional file 1: Figure S3e, f; Additional file 2: Table S11, 12). Based on the transcriptome analysis, it is likely that cell wall polysaccharide metabolism plays a role in the response of *B. napus* to waterlogging stress.

Waterlogging stress altered cell wall structure and polysaccharide contents in root

The cell wall serves as an important barrier for plants to resist external adversity stress [18, 31]. Our transcriptome analysis revealed its involvement in the response of *B. napus* to waterlogging stress (Fig. 2b). Under normal conditions, cell structure remained intact, and cells were closely arranged in both tolerant and sensitive varieties. However, in the sensitive variety, the cell wall was broken and the intracellular structure was partially damaged in root cells after 12 h of waterlogging. The cell wall became thinner and almost no normal cell morphology or complete intracellular structure could be observed in the sensitive variety. Similar changes in the tolerant variety appeared after 24 h of waterlogging (Fig. 3a). The primary cell wall of plants is primarily composed of cellulose, hemicellulose, and pectin, which are crucial for plant cell morphogenesis [32]. By analyzing the contents of cellulose, hemicellulose, and pectin, we found that the pectin content significantly decreased in the sensitive variety after 1 and 3 days of waterlogging, while no significant difference was observed in the tolerant variety. Additionally, the hemicellulose content significantly decreased after 1 and 3 days of waterlogging compared to the control group in both the tolerant and sensitive varieties. However, the cellulose content did not significantly change in either the tolerant or sensitive varieties after 3 days of waterlogging, although it did significantly decrease in the sensitive variety after 1 day of waterlogging (Fig. 3b-d). These findings strongly suggest that the cell wall structure and polysaccharide contents undergo significant changes in root cells in response to waterlogging, and that pectin may play a vital role in the different

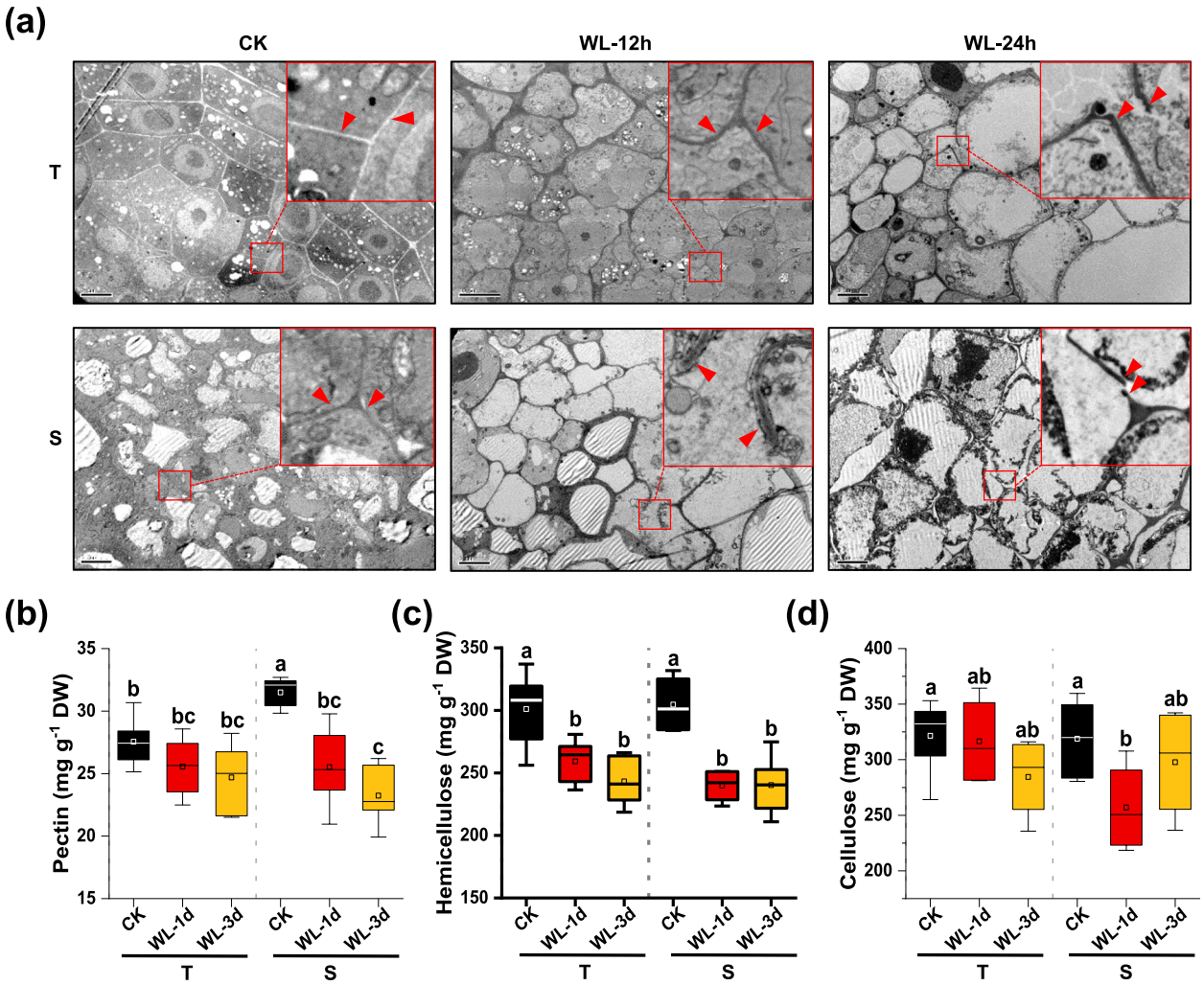

Fig. 3 Analysis of root cell wall structure and polysaccharides under waterlogging stress. **a** Ultrastructure of root tips of tolerant (T) and sensitive (S) *B. napus* varieties at 2-leaf stage under normal conditions (CK) and waterlogging (WL) for 12 h and 24 h observed by transmission electron microscopy (TEM). Bars = 2 μm. The red arrows point to the cell wall. **b** Determination of pectin content in waterlogging tolerant (T) and sensitive (S) *B. napus* varieties at 2-leaf stage under CK and WL for 1 day and 3 days. Different letters indicate significant differences, while the same letters indicate no significant differences (n = 6, one-way ANOVA for multiple comparisons, $P < 0.05$). **c** Determination of hemicellulose content in waterlogging tolerant and sensitive *B. napus* varieties at 2-leaf stage under CK and WL for 1 day and 3 days. **d** Determination of cellulose content in waterlogging tolerant and sensitive *B. napus* varieties at 2-leaf stage under CK and WL for 1 day and 3 days

responses of tolerant and sensitive *B. napus* varieties to waterlogging stress.

BnaPGIP2s reduce pectin degradation by inhibiting the activity of polygalacturonases (PGs) in response to waterlogging stress

In *B. napus*, there are five homologous *BnaPGIP2* genes, protein sequence analysis showed that there is a high similarity among *BnaPGIP2s* (Additional file 1: Figure S4a), sequence identities among *BnaPGIP2s* are more than 0.76 (Additional file 1: Figure S4b). The expression of three of the *BnaPGIP2*s (BnaA10g24080D, BnaA10g24090D, BnaC09g48700D) were up-regulated under waterlogging stress, and BnaA10g24090D showed a higher expression level in the roots of both tolerant and sensitive varieties after waterlogging for 72 h. The expression levels of *BnaA10.PGIP2* (BnaA10g24090D) and *BnaC09.PGIP2* (BnaC09g48700D) were significantly increased in the tolerant variety (Fig. 4a). On the other hand, phylogenetic analysis revealed that *BnaA10.PGIP2* closely clustered with *BnaC09.PGIP2* (Additional file 1: Figure S4c). To study the subcellular localization of BnaA10.PGIP2 and BnaC09.PGIP2, a plasma-wall separation experiment was conducted, and it was found that

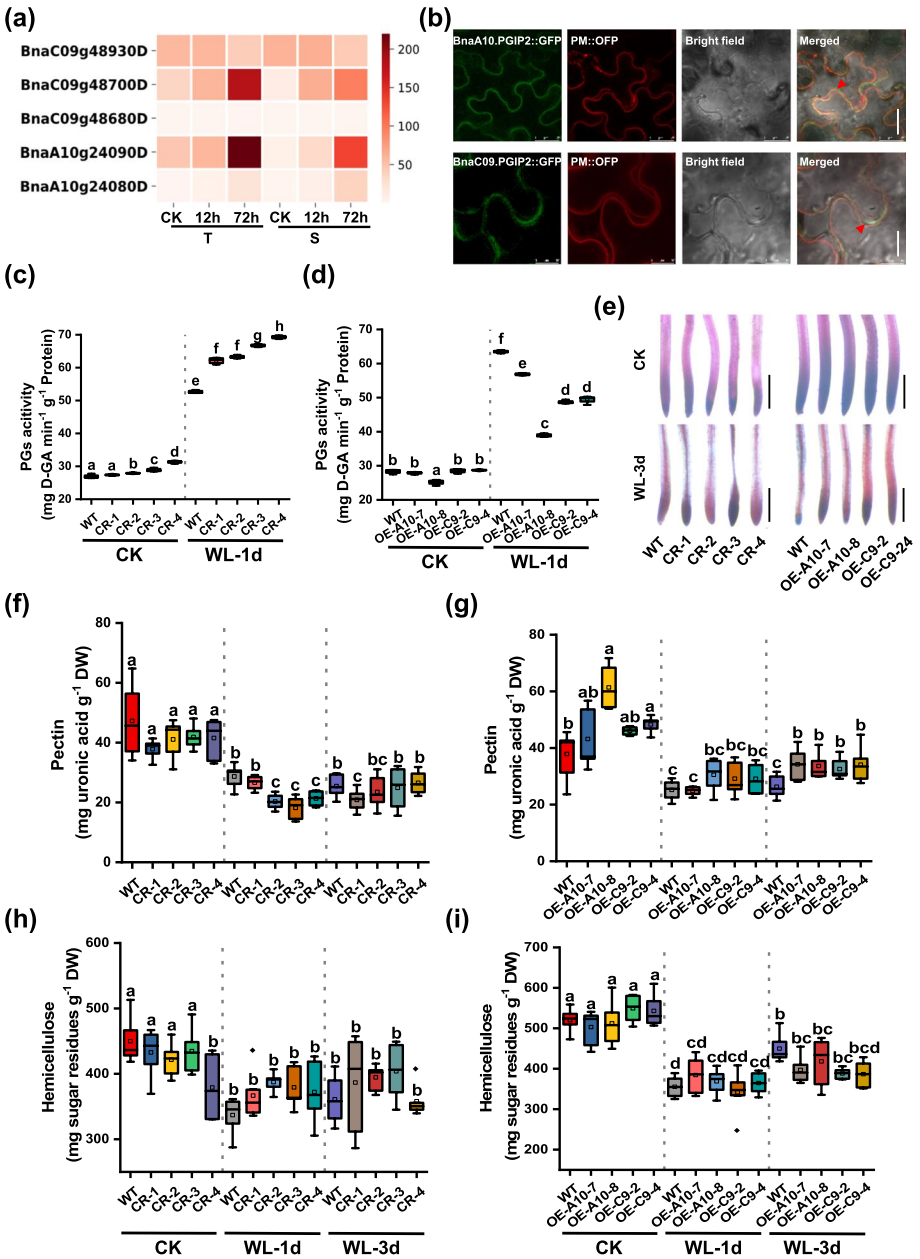

Fig. 4 BnaPGIP2s promote pectin accumulation in the root under waterlogging stress. **a** Heat map displays the expression pattern of *BnaPGIP2s* in response to waterlogging (WL) in tolerant (T) and sensitive (S) *B. napus* varieties. The redder the color bar, the higher the gene expression. It represents the expression level (TPM value) of BnaPGIP2s at 0 h, 12 h, and 72 h after root waterlogging. **b** Subcellular localization of BnaA10.PGIP2 and BnaC09.PGIP2 expressed in tobacco leaves. Cells were plasmolyzed by treatment with 0.75 mol L^{-1} mannitol for 15–20 min. Green fluorescence derived from BnaA10.PGIP2::GFP or BnaC09.PGIP2::GFP, orange fluorescence derived from membrane marker PM::OFP. The red arrowheads show BnaA10.PGIP2::GFP and BnaC09.PGIP2::GFP localized at the cell wall. Bars = 25 μm. **c** Determination of polygalacturonases (PGs) activity in *BnaPGIP2s* mutants under CK and WL for 1 day at 2-leaf stage (n = 4). **d** Determination of pectin content in *BnaPGIP2s*-overexpressing lines at 2-leaf stage under CK and WL for 1 day (n = 4). **e** Pectin level in the root tip of *BnaPGIP2s* mutants and overexpression lines at 2-leaf stage detected by ruthenium red staining under normal condition (CK) and WL for 3 days. Bars = 1 mm. **f** Determination of pectin content in *BnaPGIP2s* mutants at 2-leaf stage under CK and WL for 1 day and 3 days (n = 6). **g** Determination of pectin content in *BnaPGIP2s*-overexpressing lines at 2-leaf stage under CK and WL for 1 day and 3 days (n = 6). **h** Determination of hemicellulose content in *BnaPGIP2s* mutants under CK and WL for 1 day and 3 days (n = 6). **i** Determination of hemicellulose content in *BnaPGIP2s*-overexpressing lines at 2-leaf stage under CK and WL for 1 day and 3 days (n = 6). Different letters in the same chart indicate significant differences, while the same letters indicate no significant difference. (one-way ANOVA for multiple comparisons, $P < 0.05$)

both BnaA10.PGIP2 and BnaC09.PGIP2 were localized to the cell wall (Fig. 4b). These results were consistent with the function of PGIP2s, which participate in pectin catabolism.

To analyze the function of BnaA10.PGIP2 and BnaC09.PGIP2 in pectin catabolism under waterlogging stress, the CRISPR/Cas9 gene editing method was used to mutate the *BnaA10.PGIP2* and *BnaC09.PGIP2* genes in *B. napus*. Two sgRNA sites were designed for gene editing, with the sgRNA2 site being the off target. Based on the sgRNA1 site, single and double mutants were finally identified (Additional file 1: Figure S5a). CR-1 is the single mutant for BnaA10.PGIP2, while CR-2, CR-3, and CR-4 are the double mutants. *BnaA10.PGIP2* and *BnaC09.PGIP2* overexpression transgenic lines were also constructed in *B. napus*, respectively. qRT-PCR analysis showed that the expression of both *BnaA10.PGIP2* and *BnaC09.PGIP2* genes was significantly increased compared to the wild-type (WT) (Additional file 1: Figure S5b-c). Under normal conditions, the root PGs activity of all mutants was stronger than that in the WT, and the differences between the double mutants (CR-2, CR-3, and CR-4) and WT were significant (Fig. 4c). After 3 days of waterlogging, the differences between mutants and WT increased, and all mutants showed significantly higher root PGs activity than WT (Fig. 4c). Under normal conditions, the overexpression lines and WT had similar root PGs activity, except for the OE-A10-8 line, which showed weaker root PGs activity compared to WT (Fig. 4d). After 3 days of waterlogging, the root PGs activity of all overexpression lines was significantly lower than that in WT (Fig. 4d). To determine whether BnaPGIP2 affects polysaccharide pectin metabolism in *B. napus*, ruthenium red stain was used to directly stain the root tip. It was found that under normal conditions, the red signals in the overexpression lines were stronger, while the red signals were weaker in the mutants compared to WT, and this difference became even greater after 3 days of waterlogging (Fig. 4e). The pectin content of the single mutant (CR-1) roots showed a significant difference compared to WT after 1 day of waterlogging, and the double mutant (CR-2, CR-3, CR-4) showed significantly lower pectin content than WT after 1 day of waterlogging (Fig. 4f). The pectin content was the opposite in the overexpression lines. All overexpression lines showed an increasing trend in pectin content compared to WT under 3 days of waterlogging (Fig. 4g). The hemicellulose content showed a significant reduction after 1 day and 3 days of waterlogging compared to normal conditions in all lines, while there was no significant difference in hemicellulose content among all lines (Fig. 4h-i). These results suggest that both BnaA10.PGIP2 and BnaC09.PGIP2 confer a reduction in pectin degradation in *B. napus* roots by inhibiting the activity of PGs in response to waterlogging stress.

BnaPGIP2s improve physiological condition and enhance resistance to waterlogging stress in *B. napus*

To determine the effects of these genes, Evens Blue staining and NBT staining were performed on root tips of mutants and overexpression lines. Under normal conditions, both mutants and overexpression lines showed similar cell membrane integrity and $O_2^{\cdot-}$ levels as the wild type (Fig. 5a-b). However, after 12 h of waterlogging, the mutants exhibited greater damage to cell membranes, resulting in reduced $O_2^{\cdot-}$ production, while the overexpression lines showed the opposite phenotype (Fig. 5a-b). In terms of other physiological parameters, under normal conditions, the mutants and overexpression lines displayed similar levels of proline, malondialdehyde (MAD), and leaf water content as the wild type (Fig. 5c-h). However, after 7 days of waterlogging treatment, the proline levels in all mutants (CR-1, CR-2, CR-3, and CR-4) were higher than in the wild type, while the proline levels in all overexpression lines were lower (Fig. 5c-d). The MDA content in all mutants was higher than in the wild type, while the overexpression lines showed similar levels of proline after 7 days of waterlogging treatment (Fig. 5e-f). Leaf water content in all mutants was lower than in the wild type, with significant differences observed between the double mutants (CR-2, CR-3, and CR-4) and the wild type (Fig. 5g). Leaf water content in all overexpression lines was higher than in the wild type, whereas OE-A10-8

(See figure on next page.)

Fig. 5 BnaPGIP2s improve *B. napus* physiological condition under waterlogging stress. **a** Detection of cell membrane integrity by Evans Blue staining in the root tip of *BnaPGIP2* mutants and overexpression lines under normal condition (CK) and waterlogging (WL) for 12 h at 2-leaf stage. Bars = 1 mm. **b** Measurement of $O_2^{\cdot-}$ in the root tip of *BnaPGIP2s* mutants and overexpression lines by NBT staining under CK and WL for 12 h at 2-leaf stage. Bars = 1 mm. **c** Measurement of proline content in the root of *BnaPGIP2s* mutants under CK and WL for 7 days at 2-leaf stage. **d** Measurement of proline content in the root of *BnaPGIP2s*-overexpressing lines under CK and WL for 7 days at 2-leaf stage. **e** Measurement of malondialdehyde (MDA) content in the root of *BnaPGIP2s* mutants under CK and WL for 7 days at 2-leaf stage. **f** Measurement of malondialdehyde (MDA) content in the root of *BnaPGIP2s*-overexpressing lines under CK and WL for 7 days at 2-leaf stage. **g** Measurement of leaf water content in the root of *BnaPGIP2s* mutants under CK and WL for 7 days at 2-leaf stage. **h** Measurement of leaf water content in the root of *BnaPGIP2s*-overexpressing lines under CK and WL for 7 days at 2-leaf stage. All statistical significance was determined by Student's *t*-test, n = 5, $^*P < 0.05$, $^{**}P < 0.01$

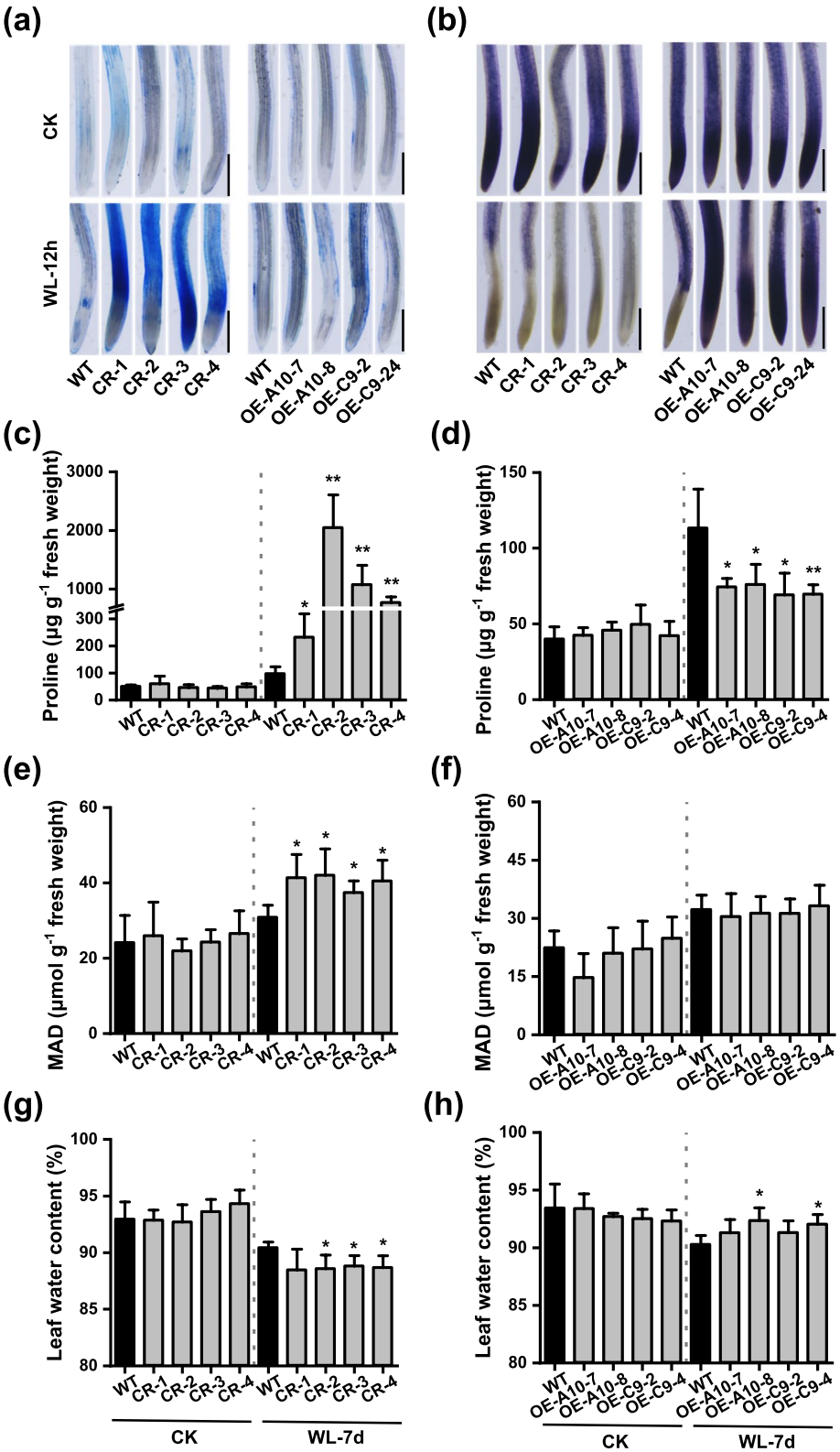

Fig. 5 (See legend on previous page.)

and OE-C09-4 showing significantly higher levels (Fig. 5h). In the absence of treatment, both mutants and overexpression lines had similar shoot fresh weight and root fresh weight compared to the control (Fig. 6a). However, after 7 days of waterlogging treatment, the shoot fresh weight and root fresh weight in the mutants tended to decrease, and the root fresh weight of the double mutants (CR-3, CR-4) significantly decreased (Fig. 6b-c). On the other hand, there was an overall increase in the overexpression lines compared to the wild type after 7

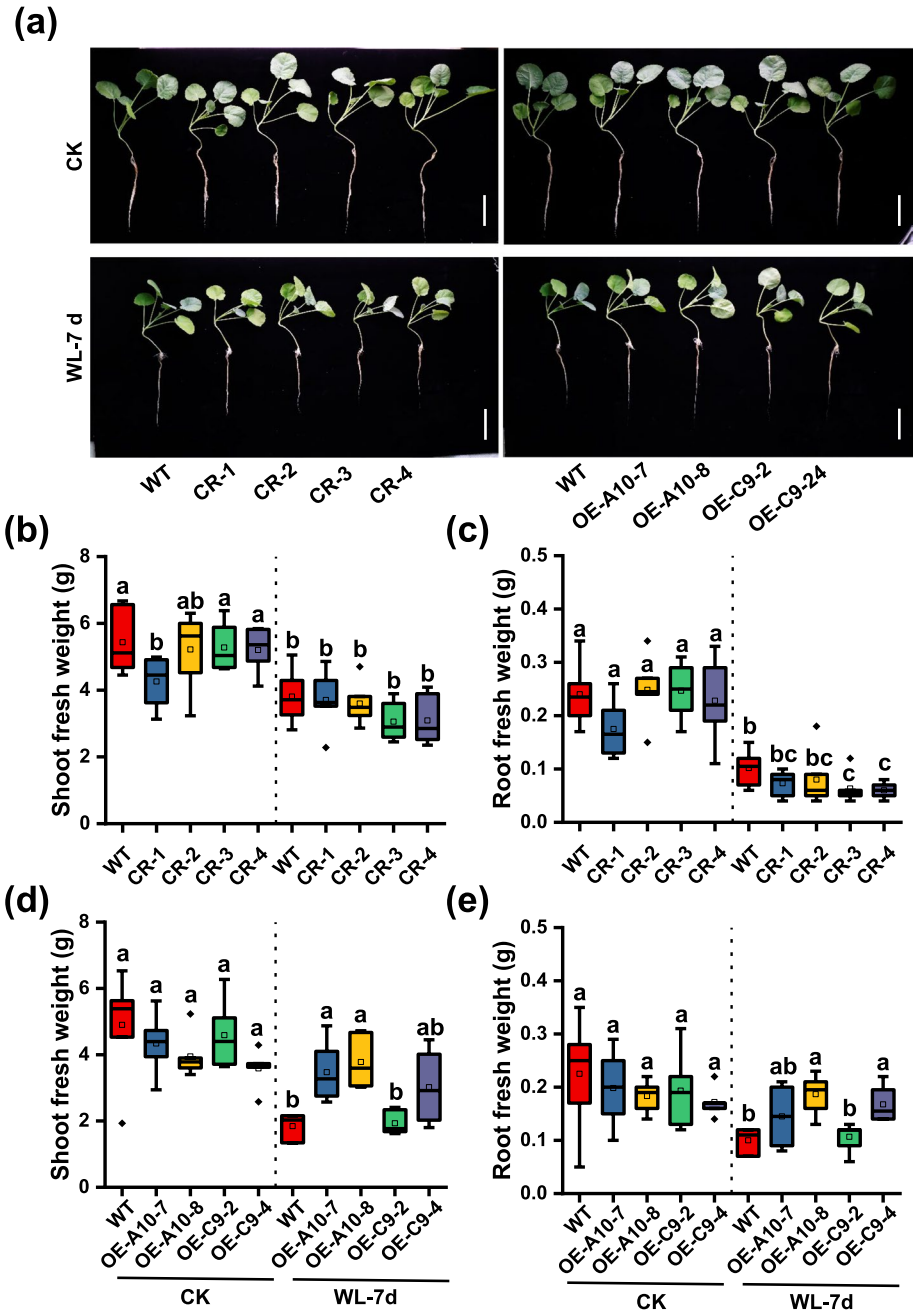

Fig. 6 *BnaPGIP2s* enhance *B. napus* resistance to waterlogging stress. **a** Identification of plant growth phenotype of *BnaPGIP2s* mutants and overexpression lines under normal condition (CK) and waterlogging (WL) for 7 days at 2-leaf stage. Bars = 5 cm. Measurement of shoot fresh weight (**b**) and root fresh weight (**c**) of *BnaPGIP2s* mutants under CK and WL at 2-leaf stage. Measurement of shoot fresh weight (**d**) and root fresh weight (**e**) of *BnaPGIP2s*-overexpressing lines under CK and WL at 2-leaf stage. Different letters in the same chart indicate significant differences, while the same letters indicate no significant difference (n = 6, one-way ANOVA for multiple comparisons, $P < 0.05$)

days of waterlogging treatment. OE-A10-7 and OE-A10-8 showed significant increases in shoot fresh weight, and OE-A10-8 and OE-C9-4 showed significant increases in root fresh weight (Fig. 6d-e). Taken together, these results suggest that both BnaA10.PGIP2 and BnaC09.PGIP2 confer waterlogging resistance to *B. napus* by reducing pectin degradation in the cell wall.

Discussion

Genetic studies on the waterlogging response of *B. napus* are still in the early stages. Previous research has shown that when subjected to waterlogging, a significant number of genes involved in leaf photosynthesis experience down-regulation, while genes related to scavenging reactive oxygen species (ROS), protein degradation, early decay, and biotic stress response pathways are heavily up-regulated [33]. Moreover, when germinating *B. napus* seeds are exposed to waterlogging, both tolerant and sensitive materials show transcriptional regulation responses. These responses involve cell wall structural components, metabolism of reactive oxygen species, antioxidant metabolism, and other central metabolic pathways. Differences in flooding tolerance phenotypes among the materials may be attributed to variations in hormone response, organic matter response, actin response, and microtubule activity [30]. In this study, a comparison of transcript level changes in response to waterlogging between tolerant and sensitive varieties revealed that certain genes involved in transcriptional regulation, material translocation, and carbon metabolism in the root of the sensitive variety overlapped with some of the genes in the root of the tolerant variety (Fig. 3a, b). The analysis also identified numerous genes associated with physiological and metabolic processes, such as hormone synthesis and response, photosynthesis and energy material transport, abiotic stress response, and ROS scavenging (Fig. 3c, d). Consequently, the transcriptome has been recognized as a crucial tool in recent years for uncovering the genetic mechanisms underlying damage response in *B. napus*.

When *B. napus* is subjected to waterlogging stress, the root system is the first to be affected, and it is the most crucial organ that suffers damage. The development of roots is hindered, and their functions are inhibited. Moreover, soluble sugars and starch reserves in the roots are rapidly depleted, resulting in the production of harmful substances like acetaldehyde. This compromises the energy supply, membrane integrity, and ion transport in the roots [34–37]. In our study, we also observed the damage caused by waterlogging stress to the root system of *B. napus*. Waterlogging for a duration of more than 12 h resulted in physiological changes in the roots (Fig. 1d), as well as damage to the cell wall and degradation of intracellular tissues and organelles (Fig. 1c and Fig. 2). As the duration of waterlogging stress increased, the normal functioning of the aboveground parts of the plant was affected, leading to reduced photosynthesis, premature leaf senescence, and even plant death [38–40]. In our study, we found that the inhibition of roots and the severity of cell membrane damage were greater in the sensitive variety compared to the tolerant variety (Fig. 1a-b). This suggests that the stability of the root structure could potentially enhance the tolerance of *B. napus* and elucidate the reasons for the disparity in tolerance between these two extreme varieties.

The role of cell wall in stabilizing root structure and function under waterlogging conditions has been demonstrated, but there is limited research on the mechanism by which the cell wall participates in waterlogging regulation. The primary plant cell wall primarily consists of cellulose, hemicellulose, and pectin, which are all structural polysaccharides [13, 14]. Previous studies have shown that changes in the cell wall during biotic stress are due to alterations in polysaccharide fractions and are achieved by regulating the cross-linking between cellulose, lignin, and pectin polymers [15]. Several enzymes involved in cell wall modification, such as xyloglucan endotransglycosylase, expansin, cellulase, and pectinase, have also been identified [16–19]. Comparative transcriptome analysis has identified cell wall-related genes involved in the waterlogging response in various species [22, 23, 41]. In the root, we observed enrichment of biological processes related to cell wall synthesis, polysaccharide metabolic processes, secondary metabolic genes, and phenylpropanoid metabolic processes (Additional file 1: Figure S2a-b; Additional file 1: Figure S3; Additional file 2: Table S3, 6; Additional file 2: Table S7-12). The regulation of these genes and pathways under waterlogging conditions may result in enhanced activity of cellulase, pectinase, and xylanase, ultimately leading to changes in the root cell wall.

Pectin is a densely composed polysaccharide found in the cell walls that can be altered by pectin methylesterases and polygalacturonase. It is believed to be involved in the response to waterlogging. In our study, we observed that the waterlogging-tolerant variety had a lower rate and degree of pectin decline compared to the sensitive variety (Fig. 2b). Various enzymes, such as exo- and endo-polygalacturonases (PGs), pectin transeliminase, and pectin methylesterase, have been reported to participate in the degradation of pectin [42]. Phytopathogenic fungi, bacteria, nematodes, and insects secrete PGs to break down the polygalacturonate chain in plant cell walls, but plants produce polygalacturonase-inhibiting proteins (PGIPs) to hinder their activity [20, 21]. PGIPs are vital components

of the plant defense mechanism and play a regulatory role in biotic stresses, although their function in abiotic stress is not well understood. Proteomic analysis has revealed that PGIPs respond to alfalfa *rhizobium* nodulation and salt stress in roots [43]. In *B. napus*, *BnPGIP1* and *BnPGIP2* are derived from wounded leaves. *BnPGIP1* is strongly induced by flea beetle feeding and mechanical wounding, while *BnPGIP2* is highly responsive to *S. sclerotiorum* infection [42]. In a transcriptome analysis, an Arabidopsis *FLR1* homolog encoding a polygalacturonase inhibitor was found to be up-regulated in the tolerant line and down-regulated in the sensitive line after 12 h of waterlogging in *B. napus* [41]. We discovered that waterlogging stress affects the cellulose, hemicellulose, and pectin contents in the cell wall, and the difference in pectin content in the root cell wall is correlated with the waterlogging resistance of different varieties (Fig. 2a-c). Two *BnaPGIP2s* were cloned from *B. napus*, and it was observed that these genes reduce pectin degradation by inhibiting the activity of PGs in the *B. napus* root, thus delaying damage to the root structure and function. *BnaA10.PGIP2* and *BnaC09.PGIP2* have high sequence similarity, and both of them inhibit the degradation rate of pectin in root tip cells under waterlogging, consequently postponing the growth inhibition and damage of roots caused by waterlogging (Figs. 4, 5 and 6). These two genes exhibit functional redundancy, as mutations in both genes have a greater impact on plants compared to a mutation in a single gene (Figs. 4, 5 and 6).

Conclusions

In conclusion, we observed significant differences in root integrity and function under waterlogging stress between two varieties of *B. napus*. The sensitive variety experienced more severe damage to the cell wall and cell membrane compared to the tolerant variety. Through transcriptome analysis and determination of cell wall polysaccharide content, we have discovered that cell wall polysaccharides play crucial roles in responding to waterlogging stress. Specifically, the pectin metabolic pathways may be responsible for the differing performance of the two varieties under waterlogging stress. We found two genes encoding polygalacturonase-inhibiting protein 2 (PGIP2) that are involved in pectin metabolic pathways and enhance resistance to waterlogging stress by inhibiting PGs activity and reducing root pectin degradation in *B. napus*. In summary, our results have revealed the vital role of *B. napus* root cell wall polysaccharide in responding to waterlogging stress.

Methods

Plant material and waterlogging treatment

Waterlogging-tolerant Santana, sensitive 23,651 *B. napus*, and wild-type Westar (used as the recipient material for transformation) were employed in this study. The uniform seeds were treated with 75% ethyl alcohol for 1 min and then rinsed with distilled water twice. The seeds were germinated on moist filter paper at a temperature of 24 °C until the radicles reached a length of approximately 2–5 mm. Subsequently, the germinated seeds were transferred to a greenhouse with a light–dark cycle of 16:8 h. After approximately 3 weeks of germination, when the seedlings reached the 2–3 leaf stage, they were subjected to water filling, with the water level maintained at 0.5 cm above the soil surface for a duration of 7 days.

Evans blue staining

The visualization of cytomembrane integrity was achieved by staining immediately with Evans blue solution. Root tips were carefully removed from the soil after undergoing normal growth and waterlogging treatment and were subsequently cleaned. From the collected samples, five to eight representative root tips were selected and submerged in a 0.025% (w/v) solution of Evans Blue for a duration of 10 min, as mentioned in the study conducted by Yin et al. [44]. Following this, the root tips were taken out and rinsed with pure water to eliminate any excess dye. The extent of tip staining was then examined using an optical microscope (BX53M, Olympus, Japan), which allowed for the determination of any damage incurred by the cell membrane of the root tips.

Nitro tetrazolium blue (NBT) staining

A total of 5–8 representative root tips were selected for staining with $O_2^{\cdot-}$. NBT chloride was used to react with $O_2^{\cdot-}$, resulting in the production of a dark brown substance. The root tips were then cut, rinsed, and stained in a 0.1% (w/v) NBT solution (dissolved in 50 mM Tris–HCl, pH 6.4) for 15 min. After rinsing with Tris–HCl buffer, the root tips were observed and photographed under an optical microscope (BX53M, Olympus, Japan).

Ruthenium red staining

The root tips were retrieved from the soils after normal growth and waterlogging treatment and were subsequently cleaned. Five to eight representative root tips were chosen and submerged in a 0.01% (w/v) ruthenium red staining solution for a period of 30 min [45]. Afterwards, the root tips were taken out, rinsed with distilled water to eliminate any surplus dye, and the pectin

content of the cell wall in the root tips was assessed using an optical microscope (BX53M, Olympus, Japan).

RNA extraction, library construction and sequence

The root samples from the tolerant variety (Santana) and sensitive variety (23,651) at 2-leaf stage were collected after 12 h and 72 h of waterlogging treatment for three repetitions. In each repetition, roots from three individuals were used for RNA extraction. The total RNA from each tissue was extracted using the DP432 kit (available at http://www.tiangen.com/). Extracted RNA samples were then sent to Personal Bio in Shanghai for library construction and sequencing. To enrich the mRNA, Oligo (dt) magnetic beads were used, followed by ion fragmentation to reduce the total RNA extracted to a length of 300 bp. Using reverse transcriptase and primers, the mRNA fragment served as a template for reverse transcription into cDNA. The cDNA was then used as a template to synthesize the second strand of cDNA. Once the library was constructed, library fragments underwent PCR amplification and selection to ensure they were within the 300-400 bp range. To assess the quality of the library fragments, the Agilent 2100 Bioanalyzer Biochip Analysis platform was utilized. The best quality library fragments were then subjected to Paired-end (PE) sequencing using the Illumina HiSeq platform, employing Next-Generation Sequencing (NGS) technology.

Transcriptome data analysis

Quality control was performed using the FastQC software [46], where the base quality and sample base composition were analyzed and evaluated. The sequencing linker and low-quality reads were then removed using the Trimmomatic software [47] in order to obtain clean reads data. The filtered data were compared to the *B. napus* reference genome (http://www.genoscope.cns.fr/brassicanapus/) using the HISAT2 software [48]. The transcript was subsequently assembled using the featureCounts software [49] to calculate the expression level, specifically the Transcripts Per Million (TPM) value. The DESeq2 package [50] was then utilized to screen for differentially expressed genes (DEGs).

Cell wall main components extraction, fractionation and measurement

The roots of both tolerant and sensitive varieties at 2-leaf stage were sampled for determination of cell wall component contents after 1 day and 3 days of waterlogging treatment. Six biological repetitions were performed. The extraction of crude cell wall materials and subsequent fractionation of cell wall components were conducted following the methods outlined by Yang et al. [51]. The uronic acid content in pectin was determined according to the protocol established by Blumenkrantz and Asboe-Hansen in 1973 [52]. In brief, 40 μL of pectin extracts were incubated with 200 μL of 98% H_2SO_4 (containing 0.0125 mol/L $Na_2B_4O_7{\cdot}10H_2O$) at 100 °C for 5 min. After cooling, 4 μL of m-hydroxydiphenyl (0.15% w/w) was added to the solution at room temperature. A total volume of 200 μL was aspirated, and the absorbance was measured at 520 nm using a microplate reader (Spark, Tecan Trading AG, Switzerland) after 20 min. The sugar residues in hemicellulose and cellulose were determined according to the method described by Ren et al. [53]. Briefly, 40 μL of hemicellulose or cellulose extracts were incubated with 200 μL of 98% H_2SO_4 at room temperature for 15 min, followed by incubation at 100 °C for 15 min. After cooling, a total volume of 200 μL was aspirated, and the absorbance was measured at 490 nm using a microplate reader (Spark, Tecan Trading AG, Switzerland).

Subcellular localization

The full-length CDSs of *BnaA10.PGIP2* and *BnaC09.PGIP2* in *B. napus* were cloned by using cDNA from Santana roots at 2-leaf stage after waterlogging for 1 day as the template. The gene-specific primers are PGIP-F-SpeI (5'-ACTAGTATGGATAAGACAACGACACTG-3') and PGIP-R-AscI (5'-GGCGCGCCACTTGCAACT ATCAAGAGGTG-3'). These target fragments were then ligated into the pMDC83 vector, which contains the GFP fluorescent tag. The resulting fusion vectors were used to transiently expressed in tobacco plants at 5–6 leaf stage. Single colonies of Agrobacterium tumefaciens GV3101 containing the recombinant vector pMDC83 with the target genes were collected by expanding the culture and resuspended in buffer (50 mM MES, pH 5.6, 5 mM Na_3PO_4, 1 mM acetosyringone). The bacterial solution was then injected into the tobacco leaf using an injector. After 2 days, the green fluorescence signal was observed using confocal laser scanning microscopy (FV1200, Olympus, Japan). Before observation, the cells were plasmolyzed by treatment with 0.75 mol L^{-1} mannitol for 15–20 min. The green fluorogenic signal had an excitation wavelength of 488 nm and an emission filter wavelength of 500–530 nm.

Construction and identification of *BnaA10.PGIP2* and *BnaC09.PGIP2*-overexpressing transgenic lines

The CDS sequences of the genes *BnaA10.PGIP2* and *BnaC09.PGIP2* were cloned from cDNA obtained from the Santana roots after at 2-leaf stage waterlogging for 1 d. The purified products were then ligated to the pCAMBIA1300S plasmid to construct an overexpression recombinant vector. Both genes were cloned using the same primer pair, namely PGIP2-F-BamHI (5'-CGCGGA

TCCATGGATAAGACAACGACACTG-3') and PGIP2-R-PstI (5'-AACTGCAGTTATTTGTCGTCGTCGTCC TTGTAGTCCATCTTGCAACTATCAAGAGGTG-3'). In our study, the wild-type Westar was used as the recipient material for the transformation of *B. napus*. The hypocotyl genetic transformation and tissue culture system for Agrobacterium-mediated genetic transformation of *B. napus* were employed [54].

qRT-PCR analysis was conducted in the overexpression lines to determine the expression level of *BnaPGIP2* by using quantitative primers PGIP2-QF/R (PGIP2-QF: 5'-TGTCCCTTGATCTCAGCAGG-3'; PGIP2-QR: 5'-GGAGAGCTGGTTGTGTGATAGG-3'). The internal reference gene for standardization was *BnaACTIN7* (BnaC09g46850D), which was amplified using the primers BnACTIN7-F (5'-CGCGCCTAGCAGCATGAA-3') and BnACTIN7-R (5'-GTTGGAAAGTGCTGAGAG ATGCA-3'). The RNA samples were reverse transcribed using the EasyScript® One-Step gDNA Removal and cDNA Synthesis SuperMix (Beijing Transgen Biotech Co. Ltd., Beijing, China). The qRT-PCR was performed using the Perfect Start TM Green qPCR Super Mix (Beijing Transgen Biotech Co. Ltd., Beijing, China) with the CFX Connect TM Real-Time System (Bio-Rad Laboratories, Inc.CA, USA). Three technical replicates were performed for each sample, and the quantitative variation between replicates was calculated using the Δ-Δ threshold cyclic relative quantification method ($2^{-\triangle\triangle Ct}$).

Construction and identification of *BnaA10.PGIP2* and *BnaC09.PGIP2* CRISPR editing lines

In this study, we utilized CRISPR/Cas9 gene editing technology to investigate the gene function of *BnaA10.PGIP2* and *BnaC09.PGIP2*. The target sites of these genes were identified using the online website CRISPR-P (http://cbi.hzau.edu.cn/cgi-bin/CRISPR), and the corresponding target sequence (Additional file 1: Figure S5) was then amplified and ligated to the PKSE401 vector at the 5' end of the sgRNA sequence. The presence of the *Cas9* gene in the obtained CRISPR transformed lines was confirmed using primers Cas9-F/R (Cas9-F: 5'-ATGGCT CCGAAGAAGAAGAGGAAG-3'; Cas9-R: 5'-GGCCAG GAGGTTATCCAGGTCA-3'). Subsequently, the target sites of Cas9-positive lines were sequenced and identified to determine the *BnaA10.PGIP2* and *BnaC09.PGIP2* target genes. Primer pair C-PGIP-A10F/R (C-PGIP-A10F: 5'-GACACTGCTTTTGTTCTTCTTCT-3'; C-PGIP-R: 5'-CAGCTGAGCCTGAGGCTC-3') was used for the specific amplification of *BnaA10.PGIP2* target sites, while primer pair C-PGIP-C09F/R (C-PGIP-C09F: 5'-GAC ACTGCTTTTGTTCTTCTCCA-3'; C-PGIP-R: 5'-CAG CTGAGCCTGAGGCTC-3') was employed for the specific amplification of *BnaC09.PGIP2* target sites.

PGs activity analysis

The roots of both tolerant and sensitive varieties at 2-leaf stage under normal conditions (CK) and waterlogging (WL) for 1 day. Four biological repetitions were performed, and roots from three individuals were used for PGs activity analysis in each biological repetition. Plant proteins were extracted from the root according to Yang et al. [55]. The protein concentration was determined using the Modified Bradford Protein Assay Kit (Sangon Biotech Co., Ltd, Shanghai, China). For quantitative analysis of PGs activity, the 3,5-dinitrosalicylic acid method was utilized [56]. The reaction mixture consisted of 300 µl of plant protein solution (100 ng μl^{-1}), 50 µl of *Citrus* peel pectin solution (0.5% w/v), 650 µl of acetate buffer (50 mM, pH = 5.0), and 1 ml of DNS solution. The mixture was reacted at 37 °C for 1 h. A standard curve was generated using known concentrations of D-galacturonic acid. Each enzymatic measurement was performed in six replicates.

Proline determination

Leaf proline was determined following the method described by Pérez-Jiménez et al. [57], with slight modifications. Five representative individuals at 2-leaf stage were selected to determine proline levels after being subjected to normal conditions, as well as a waterlogging treatment for 7 days. Approximately 0.1 g of leaf tissue was placed into a 5 mL solution of sulfosalicylic acid (3% w/v) and incubated at 100 °C for 30 min to extract the proline. Next, 2 mL of the proline extraction solution, 2 mL of glacial acetic acid, and 2 mL of acid ninhydrin were transferred into a clean 10 mL tube. The mixture was then incubated at 100 °C for an additional 30 min. After cooling, 4 mL of toluene was added to the solution to facilitate the transfer of the pigment into the toluene phase. The absorbance of the reaction solution was measured at a wavelength of 520 nm using a spectrophotometer (UH5300, HITACHI, Japan).

Malondialdehyde (MDA) determination

The determination of Leaf MDA was conducted according to Liu et al. [58], with slight modifications. Five representative individuals at 2-leaf stage were selected and subjected to normal conditions and a 7-day waterlogging treatment for MDA determination. Approximately 0.1 g of leaves were ground in a pre-cooled mortar and placed in a 5 mL solution of trichloroacetic acid (5% w/v). The resulting mixture was centrifuged at 4 °C for 10 min. In a clean 10 mL tube, 2 mL of MDA extracting solution and 2 mL of thiobarbituric acid (0.67% w/v) were mixed together and incubated at 100 °C for 30 min. After centrifugation, the absorbance of the reaction solution was measured at wavelengths of 450 nm, 532 nm, and 600 nm

using a spectrophotometer (UH5300, HITACHI, Japan). The concentration of MDA was calculated using the following formula: $C_{MDA} = 6.45*(A532-A600)-0.56*A450$.

Abbreviations

B. napus	*Brassica napus* L.
CuAO	*Copper amine oxidase*
DEG	Differentially expressed gene
MDA	Malondialdehyde
NBT	Nitro Blue Tetrazolium
PCD	Programmed cell death
PG	Polygalacturonase
PGIP2	Polygalacturonase-inhibiting protein 2
PME	*Pectin methylesterase*
TEM	Transmission electron microscopy
WL	Waterlogging
WT	Wild-type
XET	Xyloglucan endotransglycosylase

Supplementary Information

The online version contains supplementary material available at https://doi.org/10.1186/s12915-024-01972-4.

Additional file 1: Figures S1-S5. Figure S1 Experimental sample correlation analysis. Figure S2 Mclust clustering of DEGs and GO enrichment analysis in *B. napus* root. Figure S3 Mfuzz clustering of DEGs and GO enrichment analysis in *B. napus* root. Figure S4 Sequence alignments, sequence identity description and phylogenetic analysis. Figure S5 Identification of *BnaPGIP2* mutants and overexpression lines.

Additional file 2: Tables S1- S12. Table S1 List of up-regulated differentially expressed genes in *B. napus* root under waterlogging stress. Table S2 List of down-regulated differentially expressed genes in *B. napus* root under waterlogging stress. Table S3 GO enrichment analysis of mclust-cluster 2 genes in root. Table S4 GO enrichment analysis of mclust-cluster 14 genes in root. Table S5 GO enrichment analysis of mclust-cluster 3 genes in root. Table S6 GO enrichment analysis of mclust-cluster 9 genes in root. Table S7 GO enrichment analysis of mfuzz-cluster 2 genes in root. Table S8 GO enrichment analysis of mfuzz-cluster 4 genes in root. Table S9 GO enrichment analysis of mfuzz-cluster 3 genes in root. Table S10 GO enrichment analysis of mfuzz-cluster 9 genes in root. Table S11 GO enrichment analysis of mfuzz-cluster 7 genes in root. Table S12 GO enrichment analysis of mfuzz-cluster 10 genes in root.

Additional file 3. Supporting data values.

Acknowledgements
Not applicable.

Authors' contributions
Xuan Yao and Liang Guo designed and supervised this study. Jijun Li, Yuting Zhang, Yahui Chen, Yijing Wang and Zhihua Zhou performed the experiments or analyzed the data. Jijun Li and Yuting Zhang prepared the manuscript. Xuan Yao, Liang Guo, Jinxing Tu, Jijun Li, Yuting Zhang, Yahui Chen, Yijing Wang and Zhihua Zhou revised the manuscript. All the authors read and approved the manuscript.

Funding
This work was supported by grants from the Joint Funds of the National Natural Science Foundation of China (U23A20194), National Key R&D Program of China (2022YFD1200400), Key Research and Development Plan of Hubei Province (2021ABA011), Hubei Hongshan Laboratory (2021HSZD004).

Availability of data and materials
All data generated or analyed during this study are included in this published article, its supplementary information files and publicly available repositories. All RNA-seq data used for the analysis in this study have been deposited into the National Center for Biotechnology Information database (BioProject ID: PRJNA1135889) [58]. Supporting data values for $n < 6$ individual data values reported in the figures are detailed in the Additional file 3: Supporting data values file.

Declarations

Ethics approval and consent to participate
Not applicable.

Consent for publication
Not applicable.

Competing interests
The authors declare that they have no competing interests.

Received: 26 February 2024 Accepted: 5 August 2024
Published online: 02 September 2024

References

1. Fukao T, Barrera-Figueroa BE, Juntawong P, Peña-Castro JM. Submergence and waterlogging stress in plants: a review highlighting research opportunities and understudied aspects. Front Plant Sci. 2019;10:340.
2. Setter TL, Waters I. Review of prospects for germplasm improvement for waterlogging tolerance in wheat, barley and oats. Plant Soil. 2003;253:1–34.
3. Blom CWPM, Voesenek LACJ. Flooding: the survival strategies of plants. Trends Ecol Evol. 1996;11:290–5.
4. Panozzo A, Dal Cortivo C, Ferrari M, Vicelli B, Varotto S, Vamerali T. Morphological changes and expressions of *AOX1A*, *CYP81D8*, and putative *PFP* genes in a large set of commercial maize hybrids under extreme waterlogging. Front Plant Sci. 2019;10:62.
5. Song XT, Ju XT, Topp CF, Rees RM. Oxygen regulates nitrous oxide production directly in agricultural soils. Environ Sci Technol. 2019;53:12539–47.
6. Houston K, Tucker MR, Chowdhury J, Shirley N, Little A. The plant cell wall: a complex and dynamic structure as revealed by the responses of genes under stress conditions. Front Plant Sci. 2016;7:984.
7. Novaković L, Guo T, Bacic A, Sampathkumar A, Johnson KL. Hitting the wall-sensing and signaling pathways involved in plant cell wall remodeling in response to abiotic stress. Plants. 2018;7:89.
8. Peng YJ, Zhou ZX, Tong RG, Hu XY, Du KB. Anatomy and ultrastructure adaptations to soil flooding of two full-sib poplar clones differing in flood-tolerance. Flora. 2017;233:90–8.
9. Sarkar P, Niki T, Gladish DK. Changes in cell wall ultrastructure induced by sudden flooding at 25 C in *Pisum sativum* (Fabaceae) primary roots. Am J Bot. 2008;95:782–92.
10. Imene R, Haythem M. Mechanisms of aerenchyma formation in maize roots. Afr J Agr Res. 2019;14:680–5.
11. Kacprzyk J, Burke R, Schwarze J, McCabe PF. Plant programmed cell death meets auxin signalling. FEBS J. 2022;289:1731–45.
12. Ni XL, Gui MY, Tan LL, Zhu Q, Liu WZ, Li CX. Programmed cell death and aerenchyma formation in water-logged sunflower stems and its promotion by ethylene and ROS. Front Plant Sci. 2019;9:1928.
13. Aspinall GO. Chemistry of cell wall polysaccharides. In: Preiss J, editor. Carbohydrates: Structure and function. Amsterdam: Elsevier; 1980. p. 473–500.
14. Heredia A, Jiménez A, Guillén R. Composition of plant cell walls. Zeitschrift für Lebensmittel-Untersuchung und Forschung. 1995;200:24–31.
15. Kaashyap M, Ford R, Kudapa H, Jain M, Edwards D, Varshney R, et al. Differential regulation of genes involved in root morphogenesis and cell wall modification is associated with salinity tolerance in chickpea. Sci Rep. 2018;8:1–19.
16. Li C, Liu D, Lin Z, Guan B, Liu D, Yang L, et al. Histone acetylation modification affects cell wall degradation and aerenchyma formation in wheat seminal roots under waterlogging. Plant Growth Regul. 2019;87:149–63.
17. Majda M, Robert S. The role of auxin in cell wall expansion. Int J Mol Sci. 2018;19:951.

18. Peng ZZ, Liu GS, Li HL, Wang YX, Gao HY, Jemrić T, et al. Molecular and genetic events determining the softening of fleshy fruits: A comprehensive review. Int J Mol Sci. 2022;23:12482.
19. Rajhi I, Yamauchi T, Takahashi H, Nishiuchi S, Shiono K, Watanabe R, et al. Identification of genes expressed in maize root cortical cells during lysigenous aerenchyma formation using laser microdissection and microarray analyses. New Phytol. 2011;190:351–68.
20. Li HY, Smigocki AC. Wound induced *Beta vulgaris* polygalacturonase-inhibiting protein genes encode a longer leucine-rich repeat domain and inhibit fungal polygalacturonases. Physiol Mol Plant P. 2016;96:8–18.
21. Wang ZR, Chen Y, Wan LL, Xin Q, Dong FM, Zhang XH, et al. Overexpression of *OsPGIP2* confers *Sclerotinia sclerotiorum* resistance in *Brassica napus* through increased activation of defense mechanisms. J Exp Bot. 2018;69:3141–55.
22. Butsayawarapat P, Juntawong P, Khamsuk O, Somta P. Comparative transcriptome analysis of waterlogging-sensitive and tolerant zombi pea (*Vigna vexillata*) reveals energy conservation and root plasticity controlling waterlogging tolerance. Plants. 2019;8:264.
23. Zaman MSU, Malik AI, Erskine W, Kaur P. Changes in gene expression during germination reveal pea genotypes with either "quiescence" or "escape" mechanisms of waterlogging tolerance. Plant Cell Environ. 2019;42:245–58.
24. Ploschuk RA, Miralles DJ, Colmer TD, Ploschuk EL, Striker GG. Waterlogging of winter crops at early and late stages: impacts on leaf physiology, growth and yield. Front Plant Sci. 2018;9:1863.
25. Wollmer AC, Pitann B, Mühling KH. Waterlogging events during stem elongation or flowering affect yield of oilseed rape (Brassica napus L.) but not seed quality. J Agron Crop Sci. 2018;204:165–74.
26. Zou XL, Hu CW, Zeng L, Cheng Y, Xu MY, Zhang XK. A comparison of screening methods to identify waterlogging tolerance in the field in Brassica napus L during plant ontogeny. PLoS One. 2014;9:e89731.
27. Zou XL, Tan XY, Hu CW, Zeng L, Lu GY, Fu GP, et al. The transcriptome of Brassica napus L. roots under waterlogging at the seedling stage. Int J Mol Sci. 2013;14:2637–51.
28. Boem FHG, Lavado RS, Porcelli CA. Note on the effects of winter and spring waterlogging on growth, chemical composition and yield of rapeseed. Field Crop Res. 1996;47:175–9.
29. Zhou WJ, Lin XQ. Effects of waterlogging at different growth stages on physiological characteristics and seed yield of winter rape (Brassica napus L.). Field Crop Res. 1995;44:103–10.
30. Li JJ, Iqbal S, Zhang YT, Chen YH, Tan ZD, Ali U, et al. Transcriptome analysis reveals genes of flooding-tolerant and flooding-sensitive rapeseeds differentially respond to flooding at the germination stage. Plants. 2021;10:693.
31. Sakamoto S, Somssich M, Nakata MT, Unda F, Atsuzawa K, Kaneko Y, Wang T, et al. Complete substitution of a secondary cell wall with a primary cell wall in Arabidopsis. Nat Plants. 2018;4:777–83.
32. Lee YH, Kim KS, Jang YS, Hwang JH, Lee DH, Choi IH. Global gene expression responses to waterlogging in leaves of rape seedlings. Plant Cell Rep. 2014;33:289–99.
33. Colmer TD, Greenway H. Ion transport in seminal and adventitious roots of cereals during O_2 deficiency. J Exp Bot. 2011;62:39–57.
34. Duhan S, Kumari A, Lal M, Sheokand S. Oxidative stress and antioxidant defense under combined waterlogging and salinity stresses. In: Hasanuzzaman M, Fotopoulos V, Nahar K, Fujita M, editors. Reactive oxygen, nitrogen and sulfur species in plants: production, metabolism, signaling and defense mechanisms. New York: Wiley; 2019. p. 113–42.
35. Sauter M. Root responses to flooding. Curr Opin Plant Biol. 2013;16:282–6.
36. Zeng FR, Konnerup D, Shabala L, Zhou MX, Colmer TD, Zhang GP, et al. Linking oxygen availability with membrane potential maintenance and K^+ retention of barley roots: implications for waterlogging stress tolerance. Plant Cell Environ. 2014;37:2325–38.
37. Drew MC. Plant injury and adaptation to oxygen deficiency in the root environment: A review. Plant Soil. 1983;75:179–99.
38. Pan JW, Sharif R, Xu XW, Chen XH. Mechanisms of waterlogging tolerance in plants: Research progress and prospects. Front Plant Sci. 2021;11:627331.
39. Repo T, Domisch T, Kilpeläinen J, Piirainen S, Silvennoinen R, Lehto T. Dynamics of fine-root production and mortality of Scots pine in waterlogged peat soil during the growing season. Can J Forest Res. 2020;50:510–8.
40. Zou XL, Zeng L, Lu GY, Cheng Y, Xu JS, Zhang XK. Comparison of transcriptomes undergoing waterlogging at the seedling stage between tolerant and sensitive varieties of *Brassica napus* L. J Integr Agr. 2015;14:1723–34.
41. Li RG, Rimmer R, Yu M, Sharpe AG, Séguin-Swartz G, Lydiate D, et al. Two *Brassica napus* polygalacturonase inhibitory protein are expressed at different levels in response to biotic and abiotic stresses. Planta. 2003;217:299–308.
42. Wang YF, Zhang P, Li L, Li D, Liang Z, Cao YM, et al. Proteomic analysis of alfalfa (Medicago sativa L.) roots in response to rhizobium nodulation and salt stress. Genes. 2022;13:2004.
43. Yin LN, Wang SW, Eltayeb AE, Uddin M, Yamamoto Y, Tsuji W, et al. Overexpression of dehydroascorbate reductase, but not monodehydroascorbate reductase, confers tolerance to aluminum stress in transgenic tobacco. Planta. 2010;231:609–21.
44. Hong Y, Xia H, Li X, Fan RY, Li Q, Ouyang ZW, et al. *Brassica napus* BnaNTT1 modulates ATP homeostasis in plastids to sustain metabolism and growth. Cell Rep. 2022;40:111060.
45. Ewels P, Magnusson M, Lundin S, Käller M. MultiQC: summarize analysis results for multiple tools and samples in a single report. Bioinformatics. 2016;32:3047–8.
46. Bolger AM, Lohse M, Usadel B. Trimmomatic: a flexible trimmer for Illumina sequence data. Bioinformatics. 2014;30:2114–20.
47. Kim D, Paggi JM, Park C, Bennett C, Salzberg SL. Graph-based genome alignment and genotyping with HISAT2 and HISAT-genotype. Nat Biotechnol. 2019;37:907–15.
48. Liao Y, Smyth GK, Shi W. featureCounts: an efficient general purpose program for assigning sequence reads to genomic features. Bioinformatics. 2014;30:923–30.
49. Love MI, Huber W, Anders S. Moderated estimation of fold change and dispersion for RNA-seq data with DESeq2. Genome Biol. 2014;15:1–21.
50. Yang JL, Zhu XF, Peng YX, Zheng C, Li GX, Liu Y, et al. Cell wall hemicellulose contributes significantly to aluminum adsorption and root growth in Arabidopsis. Plant Physiol. 2011;155:1885–92.
51. Blumenkrantz N, Asboe-Hansen G. New method for quantitative determination of uronic acids. Anal Biochem. 1973;54:484–9.
52. Ren HW, Shen JL, Pei JW, Wang ZY, Peng ZP, Fu SF, et al. Characteristic microcrystalline cellulose extracted by combined acid and enzyme hydrolysis of sweet sorghum. Cellulose. 2019;26:8367–81.
53. Dai C, Li YQ, Li L, Du ZL, Lin SL, Tian X, et al. An efficient Agrobacterium-mediated transformation method using hypocotyl as explants for *Brassica napus*. Mol Breeding. 2020;40:96.
54. Yang S, Ulhassan Z, Shah AM, Khan AR, Azhar W, Hamid Y, et al. Salicylic acid underpins silicon in ameliorating chromium toxicity in rice by modulating antioxidant defense, ion homeostasis and cellular ultrastructure. Plant Physiol Bioch. 2021;166:1001–13.
55. Hocq L, Guinand S, Habrylo O, Voxeur A, Tabi W, Safran J, et al. The exogenous application of AtPGLR, an endo-polygalacturonase, triggers pollen tube burst and repair. Plant J. 2020;103:617–33.
56. Pérez-Jiménez M, Hernández-Munuera M, Piñero MC, López-Ortega G, Del Amor FM. Are commercial sweet cherry rootstocks adapted to climate change? Short-term waterlogging and CO2 effects on sweet cherry cv. 'Burlat.' Plant Cell Environ. 2018;41:908–18.
57. Liu P, Sun F, Gao R, Dong H. RAP2.6L overexpression delays waterlogging induced premature senescence by increasing stomatal closure more than antioxidant enzyme activity. Plant Mol Biol. 2012;79:609–22.
58. Li JJ, Zhang YT, Chen YH, Wang YJ, Zhou ZH, Tu JX, et al. The roles of cell wall polysaccharides in response to waterlogging stress in *Brassica napus* L. root. Supplementary Datasets. NCBI Bioproject accession: PRJNA1135889. 2024. https://www.ncbi.nlm.nih.gov/bioproject/PRJNA1135889.

Publisher's Note